Resolution dependence and asymmetry of electron capture to the continuum spectra

W. Meckbach, I. B. Nemirovsky, and C. R. Garibotti*
Centro Atómico Bariloche,† Instituto Balseiro,‡ 8400-S.C. de Bariloche, R.N., Argentina
(Received 6 November 1980)

Velocity distributions of electrons ejected into the forward direction have been measured with proton beams of energies comprised of between 40 and 240 keV interacting with a helium-gas target. An electron spectrometer was used, which permitted us to study the shape of the resulting peaks as a function of the instrumental angular acceptance. These data are analyzed by introducing a general parametric expression for the scattering amplitude of the ionization process. Strong skewness of the electron cusps towards lower electron velocities are observed, which appear to be independent of the large variation of peak widths as determined by different angular acceptances. It is found that this skewness is important up to the closest neighborhood of the peak top and that it leads to the inclusion of an asymmetric singular behavior of the cross section. Partial peak widths at half maximum, measured towards each side of the peak top, and also the total peak width depend linearly on the transverse experimental acceptance, as given by the product of the ion velocity times the half-angle of the electron acceptance cone. The cusp skewness, defined by the ratio of the partial widths, tends to decrease at the higher ion velocities.

I. INTRODUCTION

Since its discovery[1] in 1970 the characteristic cusp-shaped peak in electron spectra produced by collisional electron transfer to the continuum (ETC) or, more specifically, "electron capture to the continuum" (ECC) of a moving ion has been investigated with increasing interest, both experimentally and theoretically. Research on this subject has been reviewed by several authors.[2]

In this work we focus our attention to the shape of "longitudinal" ECC spectra which result when the electron emission is studied in the direction of the ion beam. Our analysis deals with the reaction

$$H^+ + He \rightarrow H^+ + He^+ + e \qquad (1)$$

at proton energies (E) between 40 and 250 keV, i.e., proton velocities (v_i) between 1.3 and 3.1 a.u.

According to earlier theories[3,4] the ECC cusp is explained through a first-perturbative-order treatment of the charge-exchange amplitude. This approximation considers for the final electronic state only a Coulomb wave centered at the projectile. The resulting ECC cusps are nearly symmetric. However, later experimental evidence obtained with bare heavy projectiles at high collision energies, revealed a remarkable skewness of ECC peaks towards lower electron velocities.[5] It has been suggested that a more accurate derivation of the first Born approximation could account for the asymmetric peak at intermediate energies,[6] but this possibility has been experimentally ruled out.[7] To explain this asymmetry, allowance must be made for the distortion of the electronic state by the electron–residual-ion interaction. This effect has been approximated by including a second-order term in the Born expansion of the charge-exchange amplitude,[8] an approach which predicts negligible ECC asymmetries when singly ionized projectiles are used. However, recent experimental evidence resulted in strongly skewed ECC cusps for the $H^+ \rightarrow He$ ionization process.[9] Subsequently, a multiple-scattering formalism has been proposed[10] that describes the final state of the electron by a dynamical two-center wave function, which is essentially the product of two Coulomb waves centered at the target and the projectile. In this way a strong asymmetry of the ECC peak results for $H^+ \rightarrow H$ scattering at intermediate collision velocities.[11] We conclude that the full influence of the electron-target Coulomb interaction must be included to account for the asymmetry of ECC cusps which results in collisions of light ions at intermediate velocities.

In this work we perform a systematic experimental study of this asymmetry. As usual, we consider the ECC process in the electron velocity space ($\vec{v}$) of Fig. 1. As the cross section $d\sigma/d\vec{v}$, which can be interpreted as the electron density per unit volume in $\vec{v}$ space, diverges when $\vec{v} \rightarrow \vec{v}_i (\vec{v}' \rightarrow 0)$, experimental resolutions, that is,

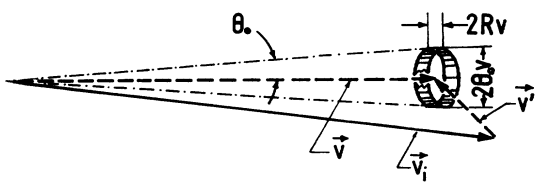

FIG. 1. The electron ($\vec{v}$) minus the ion ($\vec{v}_i$) velocity vector diagram. $\vec{v}' = \vec{v} - \vec{v}_i$. The experimental resolution is approximated by a cylinder of diameter $2\theta_0 v$ and height $2Rv$. For definition of θ_0 and R, see text.

 © 1981 The American Physical Society

the acceptances in electron velocity v (or energy E_e) and in solid angle, are decisive in determining measured peak shapes and widths. These acceptances have in Fig. 1, been represented approximately by a cylindrical "resolution volume"[12] of height $2Rv$ and diameter $2\theta_0 v$. $(\Delta v)_{\mathrm{HWHM}}/v = R$ is the experimental relative velocity resolution, which, if an electrostatic spectrometer is used, corresponds to the relative energy resolution $(\Delta E_e)_{\mathrm{HWHM}}/E_e = 2R$; θ_0 is the half-angle of the instrumental angular acceptance cone. Cusps result when $R \ll \theta_0$; then it is essentially the transverse acceptance $\theta_0 v \simeq \theta_0 v_i$ which determines their width.

It has been the usual practice to study the proportionality of ECC cusp widths to the ion velocity v_i predicted by theory,[3] but the asymmetry of these cusps has not been accounted for. The present measurements include for the first time, and through a wide range of θ_0, an investigation of cusp shapes as a function of the spectrometer angular acceptance at fixed ion velocities v_i.

We perform an interpretation of the experimental results which is independent of any particular theory. We introduce a general form of the transition amplitude which leads to a parametrization of the measured electron spectra. We show that, independently of the large changes in peak shape as resulting from our measurements with different angular resolutions, the observed asymmetry can be attributed to a proper skewness of the cross section for ECC, which is not limited to the peak tails but also appears at velocities $\vec{v} \simeq \vec{v}_i$. We also find that, in spite of this strong asymmetry, which manifests itself in that partial peak widths measured towards lower and higher electron velocities ($v \lesseqgtr v_i$) differ by a factor of about 3, the above-mentioned proportionality of total widths to $v_i\theta_0$ is approximately conserved.

II. EXPERIMENTAL METHOD AND MEASUREMENTS

A schematic drawing of our equipment is seen in Fig. 2. A proton beam, obtained from the Bariloche Cockcroft-Walton accelerator, is selected magnetically and collimated to 0.5-mm diameter and an angular divergence of less than 0.1° half-angle. It interacts with a He-gas target represented by an atomic beam emerging from the 0.25-mm bore of a hypodermic needle located, at a distance of less than 1 mm from the beam path, on the axis of a coaxial cylindrical electron spectrometer. The beam direction and the spectrometer axis enclose an angle of 42.3°. Forward-emitted electrons are deflected in the radial electric field of the spectrometer and focused back on this axis where they are allowed to traverse an orifice O_1 of 0.5-mm diameter. The focal points extended over the surface of this orifice act as the vertices of emission cones; its apex angles are determined by the diameter of one of a series of six interchangeable orifices O_2 (0.5, 1.25, 2.5, 3.75, 5.0, 6.25 mm) located at a distance of 7.16 cm from O_1 and in such a way that the angle between the direction determined by the

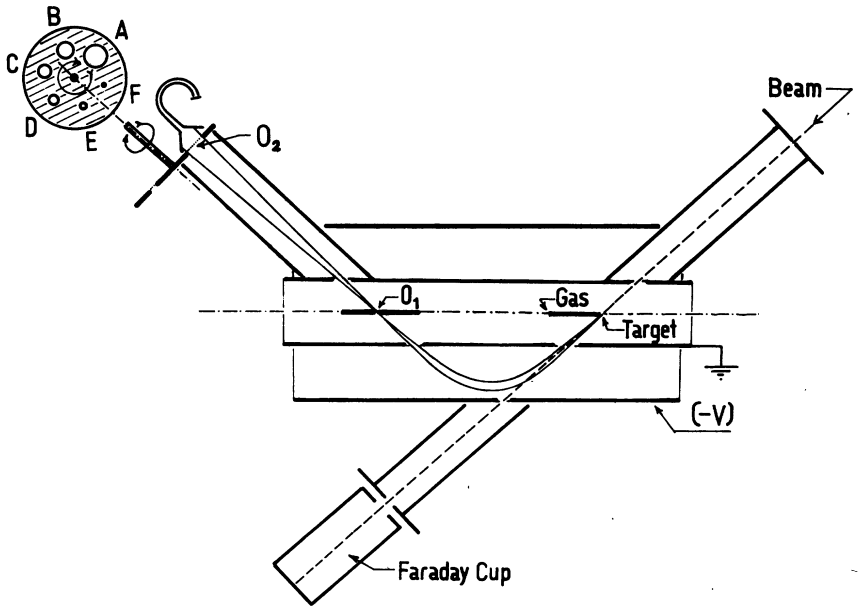

FIG. 2. Schematic diagram of the experimental arrangement ($-V$) is the spectrometer deflecting voltage. The circular orifices O_1 and O_2 determine the instrumental angular electron acceptance. O_2 is interchangeable, as shown.

centers of O_1 and O_2 and the spectrometer axis is again 42.3°. These orifices are mounted on a wheel whose axis can be turned from outside the vacuum system; hence they can easily be switched in front of the 10-mm-diameter funnel of a channeltron multiplier in which, in order to localize the energies of the detected electron close to the broad maximum of the detector efficiency dependence,[13] the funnel was maintained at a preacceleration voltage of +100 V.

Furthermore, the orifices O_2 were covered with a fine wire mesh. In this way electrostatic focusing of the impinging electrons was avoided and uniform detection of the electrons was achieved over the surfaces presented by those orifices. Then the distributions of angular acceptance of the electrons could be calculated from the geometric conditions of the apparatus as a function of an emission angle θ_a measured with respect to the axis of the accepted electron distributions (as we are measuring forward-emitted electrons, this axis is that of the ion beam). This could be simply done by considering the superposition of the two oblique circular orifices O_1 and O_2. Figure 3 shows two of these distributions which, due to the symmetry of electron paths through the spectrometer, also represent the angular acceptances as seen from the target. Each can be well approximated by a trapezoidal distribution of the same surface which determines two characteristic angles θ_1 and θ_2, as shown. A further approximation leads to a rectangular distribution which is equivalent to the acceptance cone of half-angle $\theta_0 = (\theta_1 + \theta_2)/2$, introduced by Dettman *et al.*[3] Table I shows the values of θ_1, θ_2, and θ_0 which result for the mentioned interchangeable orifices. Included in this table are also the corresponding resolutions R in electron velocity. They have been obtained from the relative energy resolutions $2R$ of the spectrometer, measured by using a heated filament electron gun. We observe from the ratios R/θ_0 that our equipment meets with the above-mentioned requirement of a flat resolution volume.

Measurements were performed with the aid of a microprocessor which, after collection of a prefixed proton-beam charge in a Faraday cup (Fig. 2), controlled the channel advance of a multiscaler simultaneously with the corresponding preselected advance of the voltage applied to the spectrometer. The electron spectra were taken in a 256-channel memory.

The working pressure in the spectrometer, with the atomic-beam target on, was about 1.2×10^{-4} torr. This pressure resulted from a reading of 2×10^{-5} torr on the ionization manometer used that, for He gas, had to be multiplied by a factor of 6.[14]

Using a path length of the proton beam between collimation aperture and target of 13 cm, it was estimated from known cross sections[15] for bound-state electron capture that no more than 0.8% of H^+ have become H^0. No quantitative information about the relative yields of ELC (electron loss to the continuum) and ECC is available for the H-He system at the energies covered in this work; consequently no evaluation of the contribution by ELC from the small fraction of H^0 in the beam to the measured spectra could be made. For 500-keV H^+ and H^0 in Ar Duncan and Menendez[16] quote that the yield from electron loss from H^0 is ≃100 times that for electron capture by H^+. On the other hand, an estimation of Rodbro and Andersen[9] for the H-He system at 60 keV results in a ratio of the differential ELC to the ECC yields of only about 3. A contribution from the repeated $H^+ \rightarrow H^0 \rightarrow (H^+ + e)$ collisional process to the measured ETC peak should depend quadratically on the gas pressure. The measured ETC signal was found to be linearly

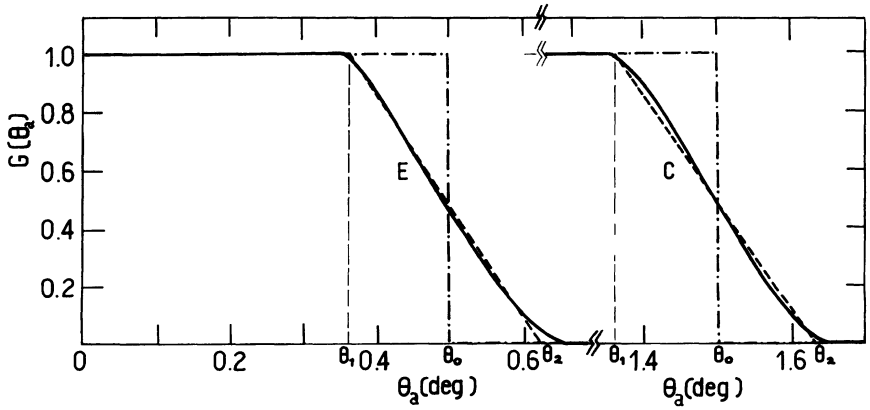

FIG. 3. Distribution $G(\theta_a)$ of angular acceptance for O_1 of 0.5-mm diam; O_2 of 1.25-mm diam (curve E) and 3.75-mm diam (curve C), respectively (see Fig. 2). The approximations of $G(\theta_a)$ by trapezoidal (θ_1; θ_2) and rectangular (θ_0) distributions are also shown.

TABLE I. Instrumental angular acceptances as determined by the electron beam defining orifices O_1 and O_2 in Fig. 2. The diameter of O_1 is 0.5 mm in all cases. The meaning of the angles θ_1, θ_2, and θ_0 is seen in Fig. 3. R is the velocity resolution (HWHM) of the spectrometer. For R and θ_0 see also Fig. 1.

Orifice O_2	Diameter of O_2 (mm)	θ_1 (deg)	θ_2 (deg)	θ_0 (deg)	θ_0 (10^{-2} rad)	R (10^{-2})	R/θ
A	6.25	2.36	2.63	2.50	4.36	0.23	0.05
B	5.0	1.86	2.14	2.00	3.49	0.21	0.06
C	3.75	1.35	1.65	1.50	2.62	0.20	0.09
D	2.5	0.85	1.15	1.00	1.75	0.16	0.09
E	1.25	0.36	0.63	0.50	0.87	0.08	0.09
F	0.5	0.02	0.32	0.17	0.29	0.04	0.14

proportional to this pressure within 5% error, indicating that single-collision conditions were met. We conclude from this evidence that a contribution from electron loss from H^0 was not detectable within our limits. We also remark that the shape, particularly the asymmetry of our measured cusps, was found to be pressure independent.

A typical spectrum is shown in Fig. 4. Note the low experimental background obtained at a base pressure of 7×10^{-7} torr, when no gas was fed into the equipment. It amounts to less than 1% of the signal in the neighborhood of the peak and about 3% at the wings. These percentages are observed for all the measured proton energies and compare favorably with those obtained in previous studies with gas targets.

In Fig. 5 we show a set of ECC cusps, normalized to 1 at the peak, obtained at $E = 191$ keV ($v_i = 2.76$ a.u.) by using the six angular acceptances of Table I. The peaks were smoothly fitted through the measured data and represented as a function of the electron energy E_e. We observe that all peaks are strongly skewed towards lower electron energies. Furthermore, as the angular acceptance varies through a wide range determined by a factor of 15 in θ_0, there is a considerable increase of the peak widths. Our measurements comprise such sets of electron spectra obtained at six different proton energies ($E_i = 43$, 72, 104, 144, 191, and 241 keV), which correspond to proton velocities $v_i = 1.31$, 1.69, 2.04, 2.76, and 3.11 a.u.

The spectra in Figs 4 and 5 are shown as measured. In the subsequent discussion these electron distributions are represented on a velocity scale. The increase of the transverse ($\simeq 2\theta_0 v$) and longitudinal ($\simeq 2Rv$) acceptances of the equipment which

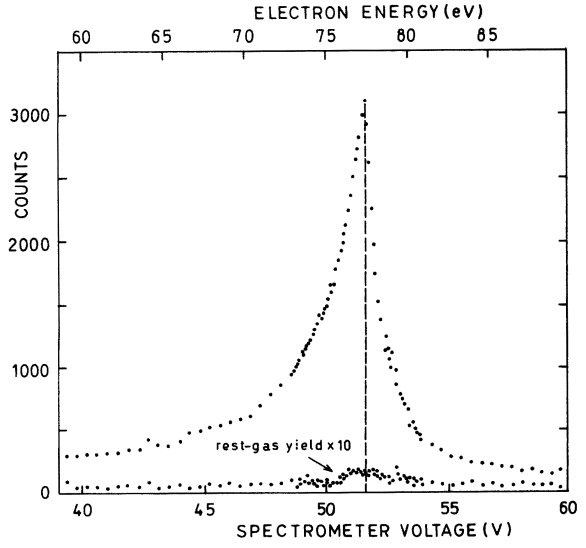

FIG. 4. Typical spectrum, taken at $E_i = 141$ keV with $\theta_0 = 0.17°$ (see Table I). Electron counts are plotted against spectrometer voltage and electron energy. The rest-gas yield must be divided by ten.

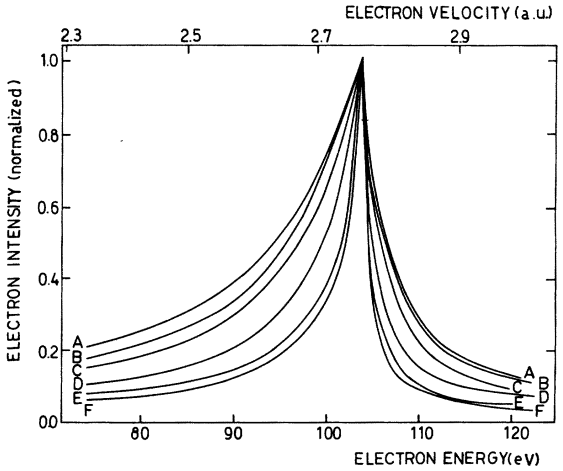

FIG. 5. Set of experimental ECC cusps obtained at $E_i = 191$ keV and for the angular acceptances contained in Table I.

result in an increase of the resolution volume (Fig. 1) with increasing electron velocity v, have been accounted for when comparing with formal cross sections. We also did not subtract any "direct ionization background" from our measured cusps because, as has been emphasized in Ref. 4, all the ejected electrons are due to a unique process, and there is no doubt that this criterion must be applied for single collisions.

III. PARAMETRIC EXPANSION OF THE CROSS SECTION

ECC cusps have usually been characterized by two parameters: height and width. This procedure is sufficient only for symmetrical peaks. However, we see in Fig. 5 that ECC cusps are strongly asymmetric and that this asymmetry appears independently of the large changes in widths, as determined by angular acceptance. It is therefore necessary to introduce more parameters to account for the observed skewness toward lower v which, as close inspection of Fig. 5 shows, is not limited to the tails of the peaks but is already remarkable in the vicinity of the peak tops ($v' \to 0$).

We proceed to a formal discussion of the observed asymmetry by introducing a general form of the transition amplitude of the ECC process which will be used for the interpretation of our experimental results.

As we are looking for $\vec{v} \simeq \vec{v}_i$ or "convoy electrons" we write the T matrix of reaction (1) in terms of $\vec{v}'$, the electron-ion velocity difference (see Fig. 1):

$$T(\vec{v}', \vec{P}, v_i) = T(v', \cos\theta', \vec{P}, v_i). \tag{2}$$

Here $\vec{P}$ is the collisional momentum transfer of the ion, v' is the modulus of $\vec{v}'$, and θ' is the angle enclosed by $\vec{v}'$ and $\vec{v}_i$, the initial ion velocity. These variables uniquely determine the transition. We expand $|T|^2$, the transition probability of the process, in a power series in v',

$$|T|^2 = \frac{1}{v'} \sum_{n=0}^{\infty} v'^n a_n(\cos\theta', \vec{P}, v_i), \tag{3}$$

The singular character, v'^{-1} of $|T|^2$ when $v' \to 0$, is explicitly shown. This behavior, which is common to all ECC theories, results from the Coulomb interaction between the emitted electron and the moving ion.

We now expand the coefficients a_n in terms of Legendre polynomials

$$a_n(\cos\theta', \vec{P}, v_i) = \sum_{j=0}^{\infty} b_j^{(n)}(\vec{P}, v_i) P_j(\cos\theta'). \tag{4}$$

The doubly differential cross section $d\sigma/d\vec{v}$ results from an integration of $|T|^2$ over the final momentum of the ion. Since the energy is conserved during the collision, the integration runs over the final projectile directions $d\Omega_P = \sin\theta_P d\theta_P d_P$:

$$\frac{d\sigma}{d\vec{v}} = (2\pi)^4 \nu^2 \frac{v_f}{v_i} \int_{\Omega_P} |T|^2 d\Omega_P. \tag{5}$$

Here ν is the reduced mass of the ion-atom system and v_f is the post-collisional ion velocity, $(v_f/v_i) \approx 1$. We finally obtain

$$\frac{d\sigma}{d\vec{v}} = \frac{1}{v'} \sum_{n,j} v'^n P_j(\cos\theta') B_j^{(n)}(v_i), \tag{6}$$

with

$$B_j^{(n)}(v_i) = 2\pi)^4 \nu^2 \frac{v_f}{v_i} \int_{\Omega_P} b_j^{(n)}(\vec{P}, v_i) d\Omega_P. \tag{7}$$

To compare with the measured distributions $Q(v, \theta)$ of ejected electrons (θ is the angle between $\vec{v}$ and $\vec{v}_i$), we must consider the spectrometer transmission function[17] $S(v, \Omega)$ and integrate $d\sigma/dv\, d\Omega = v^2(d\sigma/d\vec{v})$ over the experimental acceptances in velocity and angle:

$$Q(v, \theta) = \iint_{v\,\Omega} S(v, \Omega) v^2 \frac{d\sigma}{d\vec{v}} dv\, d\Omega. \tag{8}$$

By substituting our expansion (6) for $d\sigma/d\vec{v}$ we obtain

$$Q(v, \theta) = \sum_{n,j} B_j^{(n)}(v_i) U_j^{(n)}(v, \theta), \tag{9}$$

where

$$U_j^n = \iint_{v\,\Omega} v^2 v'^{n-1} P_j(\cos\theta') S(v, \Omega) dv\, d\Omega. \tag{10}$$

We note that for a given experimental arrangement the integrations in Eq. (10) can be performed. Then the predictions of a theoretical model of the process are contained in the coefficients $B_j^n(v_i)$ of Eq. (9).

As in the present experiment we are looking for forward-emitted electrons $\theta_a = \theta$, the integral over the azimuthal angle φ in (10) is immediate. Furthermore, as the resolution of our spectrometer can be approximated by a flat disc in $\vec{v}$ space, we can take the mean value in the v integral to obtain

$$U_j^{(n)}(v) = 4\pi R v^3 \int_{\theta_a} v'^{n-1} P_j(\cos\theta') G(\theta) \sin\theta\, d\theta. \tag{11}$$

The geometrical relations between $(v, \cos\theta)$ and $(v', \cos\theta')$ can be easily obtained from Fig. 1.

The coefficients $B_j^{(n)}$ can be obtained by fitting Eq. (9) to the measured electron distributions. In order to do this we have to introduce some restrictions in our discussion:

(a) When performing the integration in (11), the angular acceptance functions $G(\theta)$, as seen in

Fig. 3, are approximated by the trapezoidal functions defined by the angles θ_1 and θ_2, also shown in this figure.

(b) We limit our discussion to four terms in Eq. (9) by including in Eq. (3) only terms up to those linear in v' ($n=0,1$) and using in Eq. (4) only the first two Legendre polynomials ($j=0,1$). We then obtain

$$Q(v)=B_0^{(0)}U_0^{(0)}+B_1^{(0)}U_1^{(0)}+B_0^{(1)}U_0^{(1)}+B_1^{(1)}U_1^{(1)}. \quad (12)$$

Here $B_j^{(n)}=B_j^{(n)}(v_i)$ and $U_j^{(n)}=U_j^{(n)}(v)$.

The meaning of the terms contained in Eq. (12) can be understood if we look at the corresponding approximation to the cross section [Eq. (6)]:

$$\frac{d\sigma}{d\vec{v}}=\frac{1}{v'}[B_0^{(0)}(v_i)+B_1^{(0)}(v_i)\cos\theta'+v'B_0^{(1)}(v_i)+v'B_1^{(1)}\cos\theta']$$
$$=\frac{B_0^{(0)}(v_i)}{v'}+\frac{B_1^{(0)}(v_i)}{v'}\cos\theta'+B_0^{(1)}(v_i)+B_1^{(1)}(v_i)\cos\theta'. \quad (13)$$

Equation (13) contains the dependence of $d\sigma/d\vec{v}$ on θ'. For forward-emitted electrons $\cos\theta'=\pm1$ when $v\gtrless v_i$. It is obvious that the first term in Eq. (13) represents the well-known spherically symmetric electron distribution in $\vec{v}$ space[3] which, within the scope of our expansion, must be considered as a first approximation to $d\sigma/d\vec{v}$. The second term introduces an asymmetric singular behavior which is significant down to $v'=|\vec{v}-\vec{v}_i|\ll v_i$, hence $\vec{v}\simeq\vec{v}_i$. The resulting "negative" skewness may be attributed to the Coulomb attraction of the emitted electron by the residual parent ion during the collision. The remaining two terms account for the nonsingular part of the scattering amplitude and their theoretical interpretation depends on the approach used to describe the process. It is obvious that the last term introduces an additional asymmetry which tends to predominate at the tails of the electron peak. We remark that the restriction to four terms in Eq. (13) limits the validity of this equation to high and intermediate ion energies.

We can write Eq. (12) as follows:

$$Q(v)=B_0^{(0)}\left(U_0^{(0)}+\frac{B_1^{(0)}}{B_0^{(0)}}U_1^{(0)}+\frac{B_0^{(1)}}{B_0^{(0)}}U_0^{(1)}+\frac{B_1^{(1)}}{B_0^{(0)}}U_1^{(1)}\right). \quad (12')$$

It is then obvious that $B_0^{(0)}$ acts as a weight factor and that, within the approximation used, the shape of the ECC peak is determined by the remaining three coefficients.

IV. DISCUSSION

For given proton velocities v_i we have searched for the sets of four coefficients $B_j^{(n)}(v_i)$ contained in Eq. (13) by fitting Eq. (12) with the aid of a least-squares subroutine to the data contained in ensembles of electron spectra; an example was shown in Fig. 5. As for each fit six different cusps measured through the wide range in angular acceptances contained in Table I were used, strong requirements were imposed which led, at the larger v_i included in the present measurements, to a rather unique determination of these coefficients. Table II contains the coefficients that result at the proton velocities $v_i=2.04$, 2.76, and 3.11 a.u., corresponding to proton energies of $E_i=104$, 191, and 241 keV, respectively. As the fitting process was performed by using the data that correspond to cusps normalized at the top (Fig. 5), the weight factor $B_0^{(0)}$ varies with the angular acceptance.

In Fig. 6 we display as an example an experimental cusp obtained $E_i=191$ keV using a "medium" angular acceptance ($\theta_0=1°$), with the corresponding fitted cusp, as resulting from Eq. (12). Close to the peak we observe excellent agreement. Discrepancies of up to 25% are seen in the peak tails. The quality of fitting became better for the larger and worse for the smaller angular acceptances of a given set of cusps. We conclude that at sufficiently high proton energies our representation of the cross section $d\sigma/d\vec{v}$ by the four terms contained in Eq. (13) can be used to describe measured asymmetric ECC cusps.

It is interesting to observe the relative contributions of the terms contained in Eq. (12). In Fig. 7 they are shown for the case represented in Fig. 6. Near to the peak the main contribution to $Q(v)$ arises from the terms $B_0^{(0)}U_0^{(0)}$ and $B_1^{(0)}U_1^{(0)}$, the latter being responsible for the observed

TABLE II. Coefficients $B_j^{(n)}$, obtained from fitting by Eq. (12′) sets of experimental ECC cusps, as seen in Fig. 6.

Coefficients	Orifice O_2	Proton energy (keV) 241	191	104
$B_0^{(0)}$	A	0.35	0.40	0.79
	B	0.43	0.54	0.86
	C	0.56	0.73	1.4
	D	0.85	1.1	2.2
	E	1.8	2.4	5.0
	F	6.5	8.8	16.0
$B_1^{(0)}/B_0^{(0)}$		−0.18	−0.40	−0.26
$B_0^{(1)}/B_0^{(0)}$		0.09	0.38	0.09
$B_0^{(1)}/B_0^{(0)}$		−2.6	−1.3	−0.43

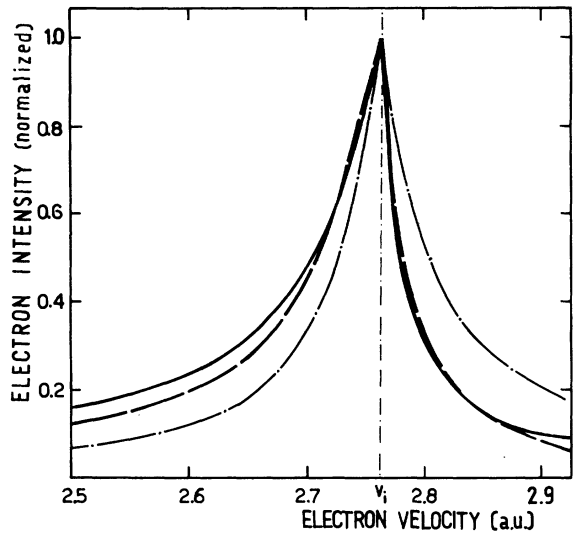

FIG. 6. ECC cusps for $E_i = 191$ keV; $\theta_0 = 1°$. (——), experiment. (– –), fitted cusps as resulting from Eq. (12). (–·–), fitted cusp with $B_0^1 = B_1^0 = B_1^1 = 0$.

strong asymmetry. These two terms could be sufficient to describe $Q(v)$ in a close neighborhood of v_i, which widens as v_i increases. The relative contribution from the remaining two terms becomes progressively more important as we proceed to the far wings of the peak.

In order to test the consistency of our fitting process we introduced a fifth coefficient $B_1^{(2)}$

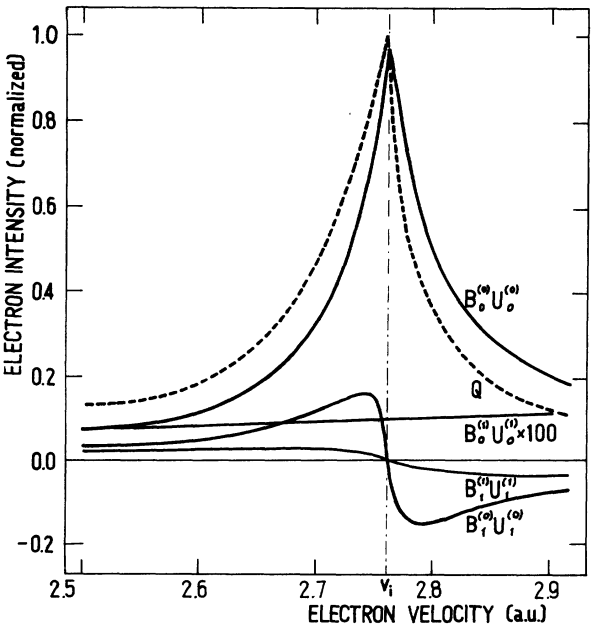

FIG. 7. Contributions of the terms in Eq. (12) to the fitted cusps $Q(v)$. Note that the peak of Q is shifted to a velocity slightly lower than v_i.

which, in Eq. (3) would correspond to the inclusion of the quadratic term in v'. By doing this at the higher proton energies (241 and 191 keV) a significant change was produced only in the values of $B_0^{(1)}$ and $B_1^{(1)}$, while a variation of less than 20% resulted in the coefficients $B_0^{(0)}$ and $B_1^{(0)}$, which correspond to the singular terms in Eq. (13). We conclude that a better fitting in the far peak tails would have required the inclusion of additional parameters. This became more evident at the lower proton energy (104 keV) where the precision of the fitting, as given by the least-squares function, was less accurate. For the lowest proton energies used in the present experiment it was not possible to fit each set of six cusps, as measured with the angular acceptances specified in Table I, with a single set of parameters.

In Fig. 6 we have also drawn for comparison the cusp obtained by letting $B_0^{(1)} = B_1^{(0)} = B_1^{(1)} = 0$, from the first term in Eq. (12) only. It results if, instead of Eq. (13), the simplified symmetric cross section

$$\frac{d\sigma}{d\vec{v}} \propto \frac{1}{v'} \tag{14}$$

of Dettmann *et al.*[3] is used. As a matter of fact, if the angular acceptance in Fig. 3 had been approximated by a rectangular distribution of half-width θ_0 this term would have led to the simple expression

$$Q(v) = 2Rv\frac{d\sigma}{dv}\Big|_{\theta_0} = 2R\frac{v}{v_i}\left[(v'^2 + vv_i\theta_0^2)^{1/2} - v\right]. \tag{15}$$

As the height $2Rv$ and the radius $\theta_0 v$ of the resolution volume in Fig. 1 increase with increasing v, it is obvious that the symmetric cross section $d\sigma/d\vec{v} \propto 1/v'$ leads to a skewness of $Q(v)$ towards higher electron velocities ($v > v_i$), which is clearly observable in Fig. 7, and emphasizes the strong discrepancy with the experimental and fitted cusps whose asymmetry is towards $v < v_i$. Assuming $v \approx v_i$ in Eq. (16), Dettmann *et al.*[3] obtain

$$\frac{d\sigma}{dv}\Big|_{\theta_0} \propto \left[(v'^2 + v_i^2\theta_0^2)^{1/2} - v'\right], \tag{16}$$

which neglects the linear increase of $\theta_0 v$ with increasing v resulting in a symmetric cusp of full width at half maximum (FWHM):

$$\Delta v_D = \tfrac{3}{2} v_i \theta_0 . \tag{17}$$

Equations (17) and (18) have been much used for comparison with experimental results in gas[2,9,18] and solid targets.[2,12,19] When comparing measured cusp widths with Δv_D, one should be conscious that Eq. (16) does not strictly apply for a comparison with $Q(v)$. It can be shown that the

FWHM resulting from Eq. (15) is

$$\Delta v = \tfrac{3}{2} v_i \theta_0 \frac{1}{1-(5\theta_0)^2} = \Delta v_D \frac{1}{1-(5\theta_0)^2} . \qquad (18)$$

For the angular acceptances shown in Table I the resulting corrections to Δv_D vary between 5 and 0.2%; they have been neglected in the discussion that follows.

In the preceding discussion we have used the parameters $E_j^{(n)}$ to describe the shape of our measured asymmetric peaks. We were able to obtain the parameters only at the higher end of the proton energy range covered in our experiment. A more phenomenological description can be made by using partial widths at half maximum taken from the abscissa of the peak top towards lower (Δv_-) and higher (Δv_+) electron velocities, as well as the total peak width (FWHM): $\Delta v = \Delta v_- + \Delta v_+$. Our equipment permitted us to perform this study not only as a function of v_i, but also as a function of the angular acceptance, which, from now on, we characterize by θ_0. The relative range covered by θ_0 (Table I) is 15-fold. In terms of the width dependence on $v_i\theta_0$ this would be equivalent to an equal variation in v_i and therefore to a relative range in ion energy which would be 225-fold. We show in Fig. 8 four experimental dependences of Δv_-, Δv_+, and Δv on θ_0, as they result from the measured cusps at $v_i = 3.11$, 2.76, 2.04, and 1.31 a.u. For the two highest proton velocities we include in this figure the partial and total widths as obtained from the corresponding fitted cusps. The resulting straight lines through the origin agree quite well with the experimental widths. We also include in Fig. 8 the dependence of the total widths given by Eq. (17). Good agreement with the widths of the experimental and fitted peaks is observed. This demonstrates that in spite of the strong asymmetry of ECC cusps the discussion of their total width dependence in terms of the simple $\Delta v_D = \frac{3}{2} v_i \theta_0$ of Dettmann *et al.*,[3] that actually corresponds to symmetric cusps, is not invalidated. However, as we proceed to lower proton velocities, discrepancies become progressively more evident. In particular we observe that for $\theta_0 \to 0$ the experimental peak widths stay finite. Estimations show that the angular spread of the incoming proton beam (<0.1°) and the finite-energy resolution of the spectrometer are insufficient to explain this effect, which is most obvious at $v_i = 1.31$ a.u. where the experimental Δv_+, Δv_-, and Δv are almost independent of the angular acceptance (θ_0). We have found neither an experimental nor a possible theoretical explanation for this effect.

As our measurements permitted the study of the FWHM (Δv) of ECC cusps on both v_i and θ_0, we combined this information in Fig. 9, where we represent as a function of v_i the slope S obtained from a linear regression of all our measured $\Delta v(\theta_0)$. At larger v_i we observe a fair agreement of the experimental S values with the straight line of slope $\frac{3}{2}$, predicted by Eq. (17). We also in-

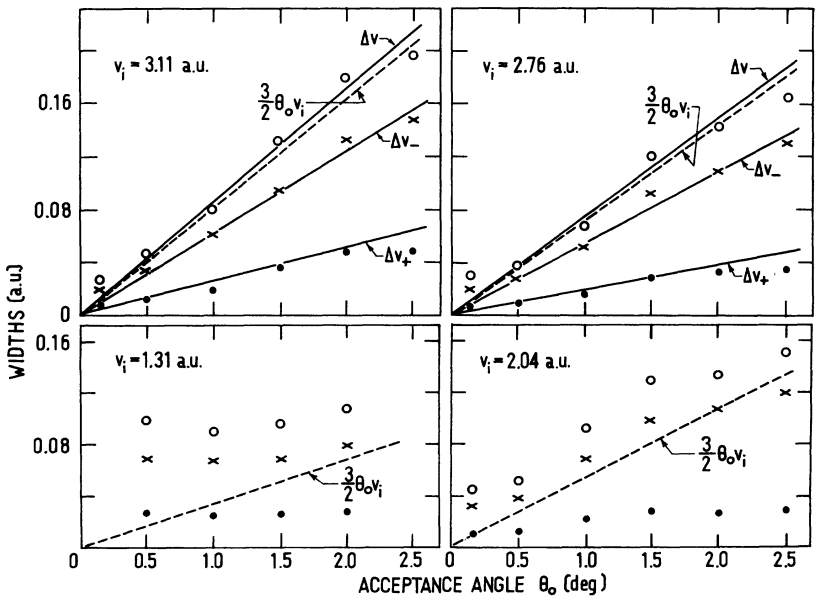

FIG. 8. Partial (Δv_-; Δv_+) and full (Δv) widths at half-height, for four proton velocities v_i, as indicated. (×) low-velocity width, Δv_-. (●) high-velocity width, Δv_+. (○) full width, Δv. (——), widths of fitted electron spectra. (---), widths from Eq. (17).

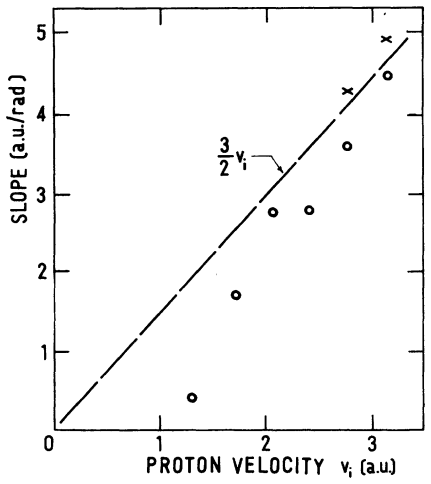

FIG. 9. Slopes S of the total peak width dependences $\Delta v(\theta_0)$, as a function of the proton velocity v_i. (○), as obtained from linear regression of experimental $\Delta v(\theta_0)$ seen in Fig. 8. (×), as obtained from fitted spectra. (— —), as resulting from Eq. (17): $S=\frac{3}{2}v_i$.

clude in this figure the slopes S which, for $v_i=3.11$ and 2.76 a.u., result from the widths of the fitted cusps. As v_i decreases the experimental slopes stay below the predicted ones. As expected from the preceding evidence this disagreement becomes very large at the lowest v_i.

Finally, we again focus our attention on the asymmetry of the measured ECC cusps, which we characterize by a "skewness" defined by the ratio of the partial widths

$$r=\Delta v_-/\Delta v_+ .$$

In Fig. 10 we present $r(\theta_0)$ for four proton velocities. It is seen that, within experimental error limits, the experimental width ratios do not depend on θ_0. This shows again, and also for ion velocities at which we did not fit the measured spectra, that the skewness of ECC cusps is independent of the large changes in widths as determined by the experimental angular acceptance, and therefore must be considered as typical for the ECC cross section.

In Fig. 11 we show the mean values of the measured width ratios as a function of v_i. This mean skewness appears to go through a maximum at $v_i \simeq 2.5$ a.u. ($E_i \simeq 150$ keV) and to decrease towards lower and higher proton velocities. This behavior is also seen in the evolution of the asymmetry coefficients (B_1^0/B_0^0) as a function of the proton energy (Table II). We include in Fig. 11 the skewness extracted from Fig. 4 of Ref. 9 which, within error limits, fits well with our results.

V. CONCLUSIONS

Our detailed study of asymmetries of ECC cusps, performed with the $H^+ \rightarrow$ He collision system and at proton velocities between 1.3 and 3.1 a.u. leads to the following conclusions. The peak asymmetries are intrinsic to the process, they do not depend on the angular resolution of the spectrometer used. A divergent asymmetric term in the scattering amplitude and not simply the smooth ionization contribution to the cross section provides the main explanation for the observed skewness. Such a term is contained in recent theoretical discussions of ECC for the $H^+ \rightarrow H$ system.[8,11]. An important result is the confirmation of the evidence that even for bare ions of charge 1 (protons) the skewness towards lower electron velocities is remarkable. This result, which is in accordance with a recent multiple-scattering theory,[11] appears to be rather natural because, when the colliding partners separate, for projectiles of low Z the interaction of the residual ion with the electron becomes relatively more important.

Furthermore, we observe that, towards the higher v_i covered in our study, the skewness, defined by the ratio of the partial peak widths

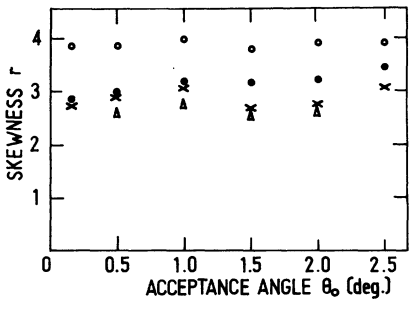

FIG. 10. Dependence of peak skewness, defined by the ratio $r=\Delta v_-/\Delta v_+$ on the angular acceptance θ_0, shown for the proton velocities v_i. (×), 3.11; ( ), 2.76; (○), 2.40, and (△), 1.31 a.u. (E_i=241, 191, 144, and 43 keV).

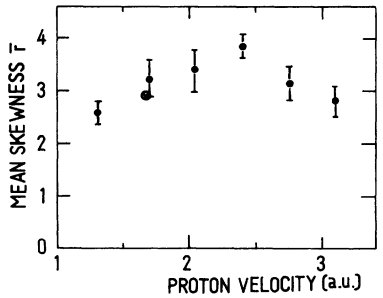

FIG. 11. Proton velocity dependence of the mean values $\bar{r}$ of peak skewness, as they result from measurements with different θ_0 (see Fig. 10). (⊗), from Fig. 4 or Ref. 9, for $\theta_0 \approx 0.36°$ only.

$(\Delta v_-/\Delta v_+)$, tends to decrease. In order to be able to perform comparisons with theoretical evidence, it would be necessary to pursue this trend by measurements performed at higher ion velocities.

In spite of the strong asymmetry of the measured ECC cusps, at not too low v_i, their total widths Δv approximately obey the proportionality to $v_i\theta_0$ contained in Eq. (17), which was originally derived for symmetric peaks.

Actually the peak skewness measured and discussed in this work for the $H^+ \rightarrow He$ system, can already be seen but subsequently, has not been accounted for in the first evidence for ECC, that is, in Fig. 2 of the pioneering paper of Crooks and Rudd.[1]

ACKNOWLEDGMENTS

The authors thank Dr. M. M. Duncan and Dr. M. G. Menéndez for their assistance in the early stage of this work. The help of Ing. G. Padín and Ing. H. Raiti in setting up the data acquisition system is gratefully acknowledged. This work was supported in part by the Cooperative Science Program between Argentina and the United States, and the Multinational Program in Physics of the Organization of the American States (OAS).

---

*Consejo Nacional de Investigaciones Científicas y Técnicas, Argentina.
†Comisión Nacional de Energía Atómica.
‡Comisión Nacional de Energía Atómica and Universidad Nacional de Cuyo.

[1]G. B. Crooks and M. E. Rudd, Phys. Rev. Lett. 25, 1599 (1970); K. G. Harrison and M. Lucas, Phys. Lett. 33A, 149 (1970).
[2]W. Meckbach and R. A. Baragiola, in *Inelastic Ion-Surface Collisions*, edited by N. M. Tolk, J. C. Tully, W. Heiland, and C. W. White (Academic, New York, 1977), p. 283; I. A. Sellin, J. Phys. (Paris), 40, C1-255 (1979); C. R. Vane, IEEE Trans. Nucl. Sci. NS-26, 1078 (1979); M. W. Lucas, in Proceedings of the Workshop on Physics with Fast Molecular-Ion Beams, edited by D. S. Gemmell, Argonne National Laboratory, Report No. ANL/PHY-79-3, p. 291; V. H. Ponce and W. Meckbach, Comments At. Mol. Phys. 10, 231 (1981).
[3]K. Dettmann, K. G. Harrison, and M. W. Lucas, J. Phys. B 7, 269 (1974).
[4]J. Macek, Phys. Rev. A 1, 235 (1970); W. J. B. Oldham, Phys. Rev. 161, 1 (1967); A. Salin, J. Phys. B 5, 979 (1972).
[5]C. R. Vane, I. A. Sellin, M. Suter, G. D. Alton, S. B. Elston, P. M. Griffin, and R. S. Thoe, Phys. Rev. Lett. 40, 1020 (1978).
[6]F. T. Chan and J. Eichler, Phys. Rev. A 20, 367 (1979); R. Shakeshaft and L. Spruch, *ibid.* 20, 376 (1979).
[7]M. Breinig, S. Elston, J. Sellin, L. Liljeby, R. Thoe, C. R. Vane, H. Gould, R. Marrus, and R. Laubert, Phys. Rev. Lett. 45, 1689 (1980).
[8]R. Shakeshaft and L. Spruch, Phys. Rev. Lett. 41, 1037 (1978).
[9]M. Rødbro and F. D. Andersen, J. Phys. B 12, 2883 (1979).
[10]C. R. Garibotti and J. E. Miraglia, Phys. Rev. A 21, 572 (1980).
[11]C. R, Garibotti and J. E. Miraglia, J. Phys. B 14, 863 (1981).
[12]W. Meckbach, K. C. Chiu, H. H. Brongersma, and J. W. McGowan, J. Phys. B 10, 3256 (1977).
[13]K. C. Schmidt, Bendix Report No. 9803 (unpublished); F. Bordoni, Nucl. Instrum. Methods 97, 405 (1971); R. L. Arnoldy, P. O. Isaakson, and D. F. Gats, Rev. Sci. Instrum. 44, 172 (1973).
[14]Leybold Heraeus, Report No. 70/AO, 15.1.2 (unpublished).
[15]S. K. Allison and M. García Muñoz, in *Atomic and Molecular Processes*, edited by D. R. Bates (Academic, New York, 1962), p. 721 ff.
[16]M. M. Duncan and M. G. Menendez, Phys. Rev. A 19, 49 (1979).
[17]F. Eagen and E. N. Sikafus, Rev. Sci. Instrum. 48, 1269 (1977).
[18]K. C. R. Chiu, J. W. McGowan, and J. B. Mitchell, J. Phys. B 11, L117 (1978).
[19]W. Steckelmacher, R. Strong, M. N, Khan, and M. W. Lucas, J. Phys. B 12, 2711 (1978); W. Meckbach, N. Arista, and W. Brandt, Phys. Lett. 65A, 113 (1978).